The Late Cretaceous Orogenic System: Early Inversion of the Neuquén Basin and Associated Synorogenic Deposits (35º–38º S)

Lucas Fennell, Pablo Borghi, Federico Martos, Eduardo Agustín Rosselot, Maximiliano Naipauer and Andrés Folguera

Abstract The first regional tectonic uplift was registered in the Neuquén Basin at ca. 100 Ma, resulting in the inception of the first foreland basin of the Andes at these latitudes. The infill of this foreland basin is represented by the nonmarine deposits of the Neuquén Group, characterized by the presence of growth strata and fold-thrust belt detrital derivation, typical of wedge-top depozones. The presence of a long-lasting hiatus and angular unconformities in structures west of the wedge-top area indicate that these constituted the main detrital source areas of the Late Cretaceous foreland basin. These structures were uplifted by tectonic inversion of pre-existing normal faults, a mechanism that was also responsible for isolated basement block uplifts detected in the foredeep depozone. The regional unconformity between the synorogenic deposits of the Neuquén Group and the back-bulge deposits of the Bajada del Agrio Group represents the migration of the forebulge, which constituted another important detrital source of the foreland basin during its mature phase. An active fold-thrust belt, disconnected basement block uplifts and the identification of the typical depozones of present foreland basins provide a complete picture of the Late Cretaceous orogenic system responsible for the early inversion of the Neuquén Basin.

Keywords Neuquén group basin · Foreland basin · Early andean uplift · Flexural subsidence · Cretaceous

1   Introduction and Geological Setting

The Late Cretaceous represents a period of important palaeogeographic reorganization in the Neuquén Basin, whose stratigraphy records the transition between a

L. Fennell (✉) · F. Martos · E. A. Rosselot · M. Naipauer · A. Folguera
CONICET—Universidad de Buenos Aires, Instituto de Estudios Andinos Don Pablo Groeber (IDEAN), Buenos Aires, Argentina
e-mail: lucasfennell90@gmail.com

P. Borghi
Wintershall Energía S. A, Buenos Aires, Argentina

retroarc extensional settings towards a contractional system at ca. 100 Ma (Vergani et al. 1995; Manceda and Figueroa 1995; Tunik et al. 2010; Balgord and Carrapa 2016; Fennell et al. 2017a). This transition is marked in the Neuquén Basin by a regional unconformity over the deposits of the Lower Cretaceous Mendoza and Bajada del Agrio Groups (Groeber 1946), and the inception of a Late Cretaceous flexural foreland basin (Ramos and Folguera 2005). The infill of this foreland basin is represented by the nonmarine red beds of the Neuquén Group and the equivalent Diamante Formation, whose different naming responds to the difficulty of making regional correlations at the moment of their definition (Groeber 1947), although these deposits nowadays can be perfectly correlated (Bettini et al. 1978; Fennell et al. 2017b). Therefore, in order to avoid unnecessary naming, these deposits will be addressed as the Neuquén Group throughout the rest of the chapter, whose study is possible due to the complex deformational scenario that affected the Neuquén Basin since the Southern Central Andes' initial uplift (Horton 2018a). Of all the morphostructural units in which the Southern Central Andes are segmented (see Folguera et al. 2016), the best exposures of these units are found in the Principal Cordillera, where the orogenic front has cannibalized and incorporated the Late Cretaceous foreland basin into the Andean wedge before reaching its current position (Fig. 1).

Together with the Huincul ridge (Silvestro and Zubiri 2008), the area comprised between 35º S and 38º S represents one of the best-known areas in terms of structural kinematic evolution along the entire Neuquén Basin (Fig. 1), in which an important Late Cretaceous component has been recognized (Orts et al. 2012; Mescua et al. 2014; Rojas Vera et al. 2015; Folguera et al. 2015; Sagripanti et al. 2016; Branellec et al. 2016; Sánchez et al. 2018). This area is characterized by the occurrence of a series of long wavelength double-plunging anticlines (Fig. 2), whose deepest level of exposure reaches the upper Palaeozoic to Lower Triassic structural basement (Llambías et al. 2007). Nonmarine deposits of the Neuquén Group are found surrounding these thick-skinned structures, although their real regional extent remains obscured by subsequent exhumation processes and the thick Cenozoic volcanic and nonmarine synorogenic cover (Silvestro et al. 2005; Silvestro and Atencio 2009; Kay et al. 2006; Horton et al. 2016). Nevertheless, by integrating field observations and isopach maps based on subsurface information (Bettini et al. 1978; Manacorda et al. 2002), a wedge-shaped geometry for the Late Cretaceous sequences becomes evident, with maximum thicknesses recorded to the west and onlapping relationships over the San Rafael Block and the North Patagonian massif to the east (Figs. 1 and 2). In order to make a complete description of the Late Cretaceous foreland basin system, the main structures in the Argentine territory between 35º–38º S were divided in three sectors: western, central and eastern sectors (Fig. 2).
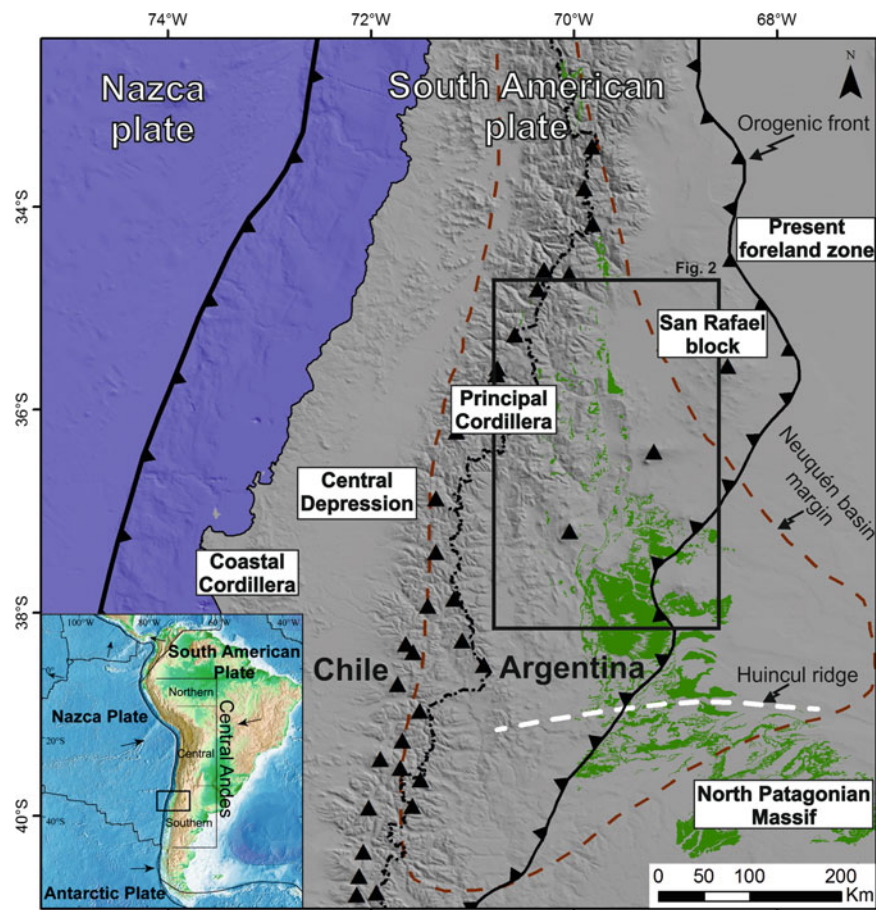
Fig. 1 Morphostructural units in which the Southern Central Andes are segmented and location of the study area within the Neuquén Basin. Outcrops of the Late Cretaceous Neuquén Group nonmarine foreland basin deposits are highlighted in green, and the location of the Neuquén Basin margin, the Huincul ridge and the current orogenic front are taken from Sagripanti et al. (2011)

2 Western Sector

Within the western sector, the northernmost analysed structure corresponds to the Río del Cobre anticline, whose backlimb exposes a ca. 100 Ma hiatus between Cretaceous units and late Eocene volcaniclastic rocks, indicating as much as 5 km of erosion (Mescua et al. 2013). Southeast of this structure, the Dedos Silla anticline presents partly eroded and condensed sections of the Late Cretaceous red beds (Legarreta and Kozlowski 1984; Mescua et al. 2013), evidencing active uplift during or after sedimentation (Branellec et al. 2016). Due to its NE trend, the southern plunge of this structure reaches the international boundary at approximately 35° 40′ S, where Lower
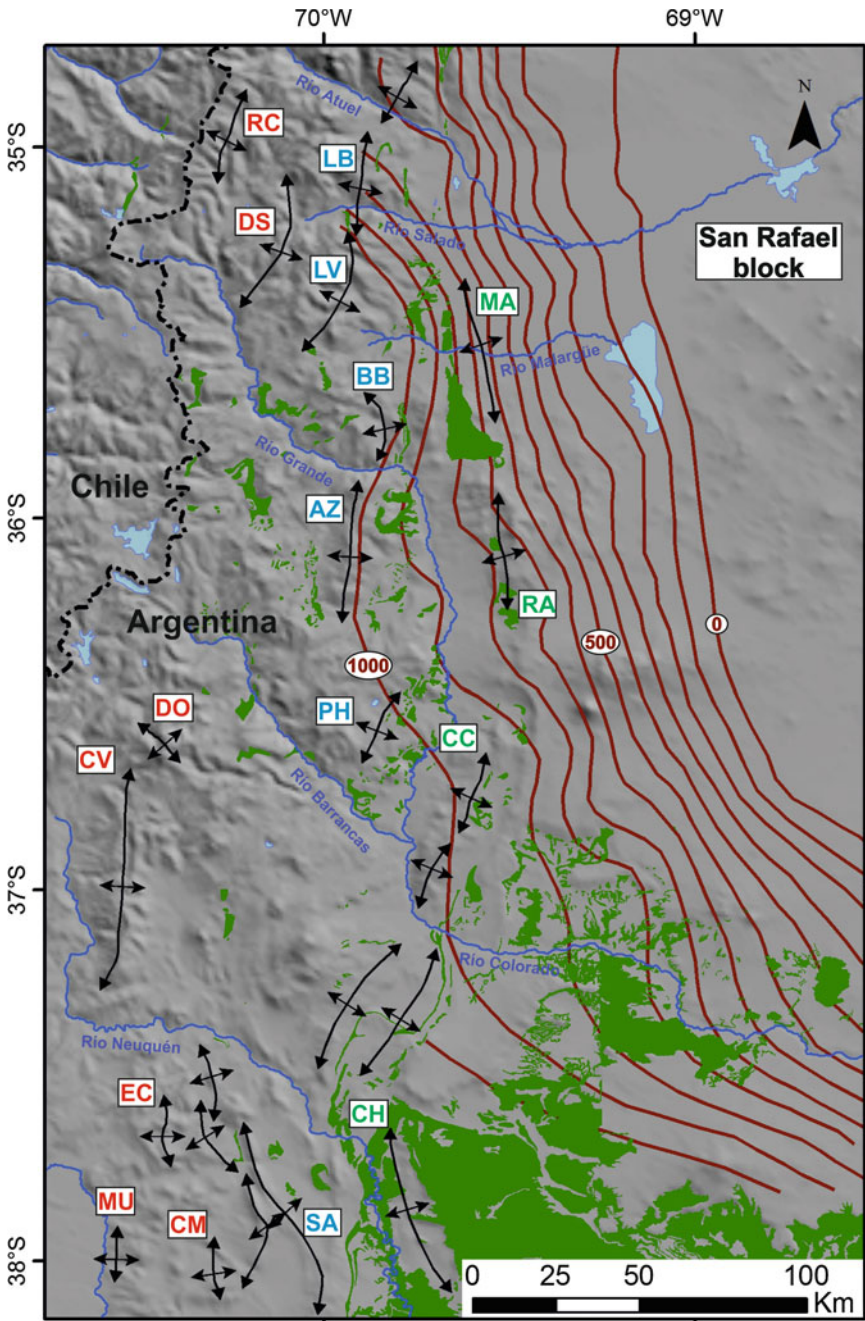
◄Fig. 2 Map showing the main structures and the wedge-shaped regional geometry of the Late Cretaceous foreland basin, as evidenced by the isopachs obtained from outcrops (in green) and subsurface information of the Neuquén Group (taken from Manacorda et al. 2002). Abbreviations in red correspond to western anticlines: RC, Río del Cobre; DS, Dedos Silla; DO, Domuyo, CV, Cordillera del Viento; EC, El Cholar; MU, Mulichinco; CM, Cerro Mocho; in blue correspond to the central anticlines: LB, Los Blancos; LV, La Valenciana; BB, Bardas Blancas; AZ, Sierra Azul; PH, Puntilla de Huincán; SA, Salado; and in green correspond to the eastern anticlines: MA, Malargüe; RA, Ranquil Co; CC, Cara Cura; CH, Chihuidos

Cretaceous marine deposits of the Mendoza Group are unconformably covered by the latest Cretaceous volcaniclastic deposits of the Los Ángeles unit (Fennell et al. 2017c; Iannelli et al. 2018), suggesting an important non-depositional or erosive event during Late Cretaceous times (Fig. 3a).

South of the Río del Cobre and Dedos Silla anticlines, an important Late Cretaceous depocentre, located between the Ríos Grande and Barrancas withholds ~1.6 km of preserved thicknesses of the Neuquén Group (Orts et al. 2012), which separates these structures from the Domuyo and Cordillera del Viento double-plunging anticlines (Fig. 2). The Cordillera del Viento anticline represents one of the best examples of Late Cretaceous structures along the entire Neuquén Basin, due to the fact that the Mendoza Group deposits are unconformably overlain by the Neuquén Group deposits in its eastern limb (Groeber 1946), while preserving an even longer hiatus in its western limb (Fig. 3b). This hiatus can be observed at 37º S along the Neuquén River, where the structural basement of the Neuquén Basin represented by the Upper Permian to Lower Triassic Choiyoi Group (Llambías et al. 2007) is unconformably overlain by the Eocene volcaniclastic rocks of the Cayanta Formation (Fig. 3b) (Jordan et al. 2001).

This structural trend is completed by the El Cholar, Mulichinco and Cerro Mocho structures (Fig. 2), whose crosscutting and unconformable relationships with latest Cretaceous to Palaeocene magmatic rocks allow their characterization as Late Cretaceous uplifted structures (Ramos 1981; Zamora Valcarce et al. 2009; Rojas Vera et al. 2015).

3 Central Sector

In the central sector, structures such as the Los Blancos and La Valenciana anticlines (Fig. 2) present numerous remnants of the Neuquén Group deposits, which due to their position respect to the western Río del Cobre and Dedos Silla structures, suggest that these could have been associated with synorogenic sedimentation during Late Cretaceous times (Mescua et al. 2014; Branellec et al. 2016). Although no growth strata have been reported in the vicinities of these structures yet, the fact that latest Cretaceous marine and lacustrine deposits of the Malargüe Group (Barrio 1990;
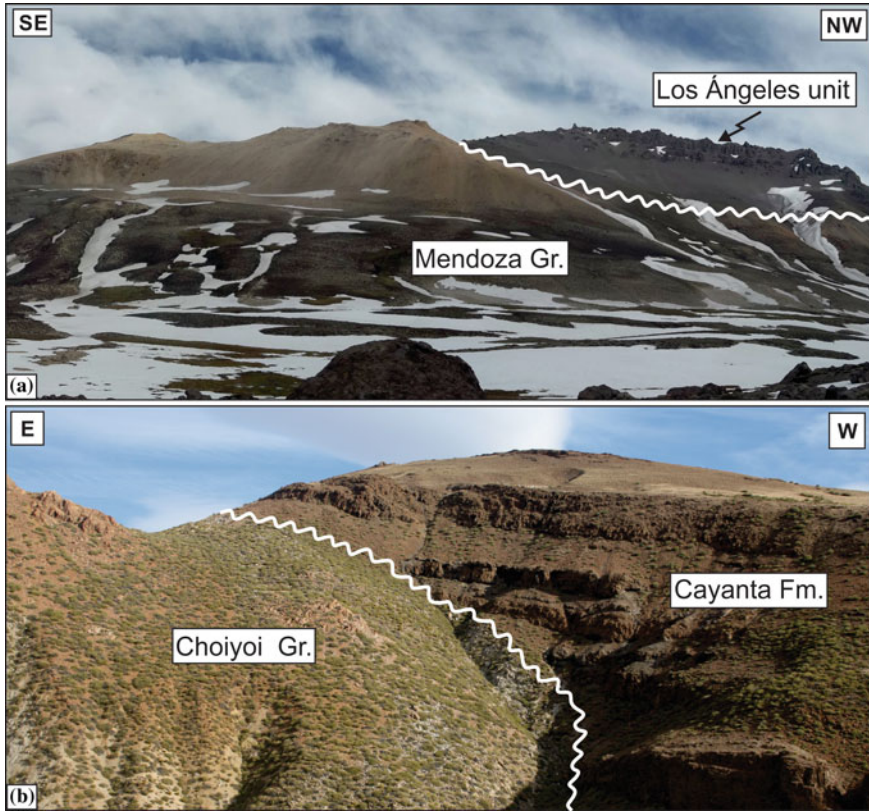
Fig. 3 a Unconformable relation between the Lower Cretaceous marine deposits of the Mendoza Group and the latest Cretaceous volcaniclastic deposits of the Los Ángeles unit near the international border between Chile and Argentina at 35º 40′ S. **b** A ca. 200 Ma hiatus is evidenced by the onlap of the Eocene volcaniclastic rocks of the Cayanta Formation over the Upper Permian to Lower Triassic crystalline rocks of the Choiyoi Group along the Río Neuquén at 37º S (Heredia, pers. comm.)

Parras and Griffin 2013) onlap against these structures indicate that these could have been positive features during Late Cretaceous times (Bettini et al. 1978).

A similar setting is observed in the Bardas Blancas anticline to the south, although the presence of growth strata associated with this structural trend documented in the Sierra Azul anticline suggests its Late Cretaceous growth (Fig. 2). In the eastern limb of the Sierra Azul anticline, Fennell et al. (2017a) identified progressive unconformities and thickness variations in the upper terms of the Neuquén Group (Fig. 4a), which are associated with seismetes preserved in associated fine-grained facies (Fig. 4b). The coarser facies of the Neuquén Group in this area are composed of limestones at the base, which are gradually replaced by acid volcanic clasts (Borghi et al. 2017) and intraclasts of the Neuquén Group towards the top (Fig. 4c). The combination of these observations, as well as the documentation of onlap relations in its western limb by Orts et al. (2012), converts the Sierra Azul anticline in one of the type examples of
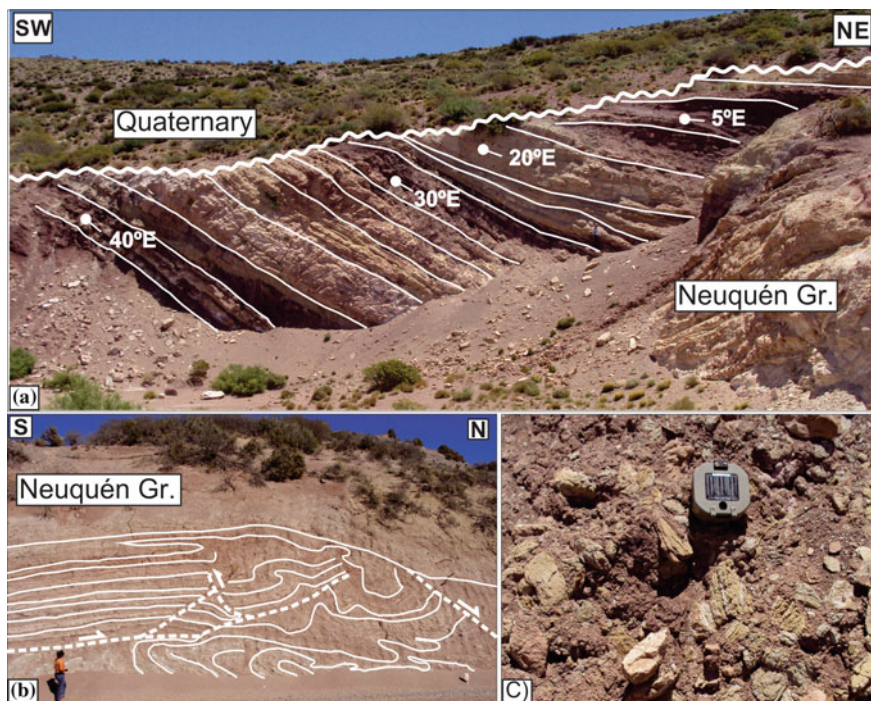
Fig. 4 **a** Growth strata in the upper terms of the Neuquén Group in the eastern limb of the Sierra Azul anticline. **b** Seismetes preserved in fine-grained facies of the Neuquén Group associated with the growth of the Sierra Azul anticline. **c** The coarser facies in the upper terms of the Neuquén Group are mainly composed of intraclasts, evidencing the progressive cannibalization of its deposits during the uplift of the Sierra Azul anticline

growing structures below the level of sedimentation during Late Cretaceous times. Although less documented given the extensive Neogene volcanic cover, the Puntilla de Huincán anticline to the south (Fig. 2) represents another example of this type of structures, where seismic profiles show thinning of the Late Cretaceous sequences towards its hinge (Galarza et al. 2009).

South of the Río Barrancas, Late Cretaceous depositional geometries and structures are covered by the voluminous Quaternary volcanic cover of the Tromen volcano (Sagripanti et al. 2016), although structures such as the Salado anticline share the behaviour with the rest of the structures within the central sector (Fig. 2). This structure in particular has been analysed by Cobbold and Rossello (2003) through a seismic profile and well data, where they show active thrusting throughout almost all of the Late Cretaceous, evidenced by the presence of a Late Cretaceous footwall basin east of the Salado anticline whose thickness exceeds by 1.8 km the thickness recorded in the hanging wall.

4 Eastern Sector

The eastern sector is represented by isolated structures whose uplift has been attributed mainly to the Cenozoic, and in particular to the last 20 Myrs (Silvestro et al. 2005; Zamora Valcarce et al. 2009; Silvestro and Atencio 2009; Sagripanti et al. 2011; Álvarez Cerimedo et al. 2013). However, evidences of uplift have been reported in many of these structures, whose spatial development coincides with major displacements in the isopachs of the Neuquén Group (Fig. 2).

The Ranquil Co anticline is the northernmost representative of these structures, where Groeber (1947) had already hinted the increasing thickness of the Neuquén Group towards both limbs of the structure (see Fennell et al. 2017b for a view of the scheme). This structure was recently inspected by Fennell et al. (2017a), confirming the thickness variations in the Neuquén Group (Fig. 5a) and detecting the presence of progressive unconformities in its core (Fig. 5b). These evidences suggest that the lower Neuquén Group deposits in this area present growth geometries, whose coarse facies are mainly composed of acid volcanic clasts (Fig. 5c), supported by sandstone petrographic descriptions (Fennell et al. 2017b).

The Cara Cura anticline to the south (Fig. 2) also presents evidences of active uplift during Late Cretaceous times, where syndepositional deformation has been reported in the coarse facies of the basal terms of the Neuquén Group (Fennell et al. 2017a). Upon closer inspection, the basal contact of the Neuquén Group in the western limb
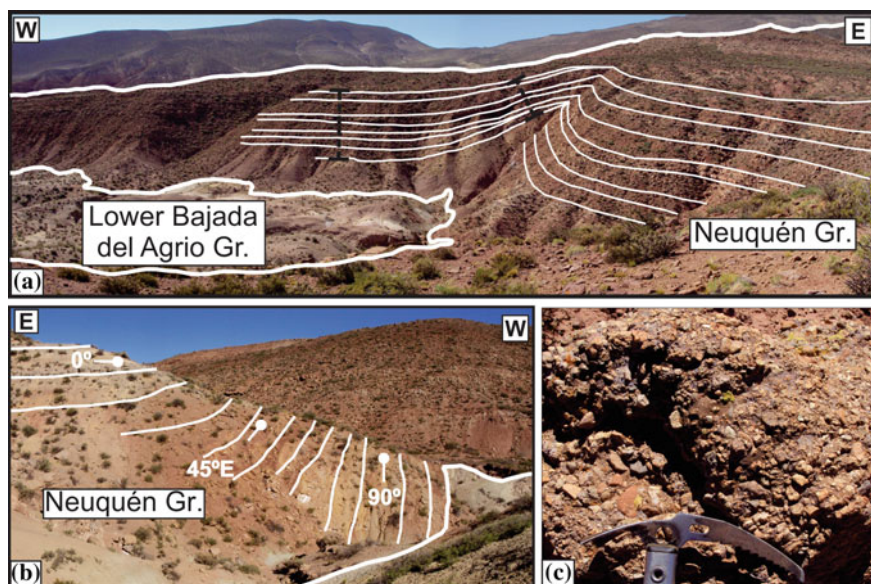

Fig. 5 a Thinning of the Neuquén Group deposits towards the hinge of the Ranquil Co anticline. **b** Progressive unconformities in the core of the Ranquil Co anticline. **c** Acid volcanic clasts dominate the coarse facies of the lower terms of the Neuquén Group in the Ranquil Co anticline

of the Cara Cura anticline is erosive and angular (Fig. 6a), highlighting the absence of the upper terms of the Bajada del Agrio Group and becoming the first description in this area of this highly documented angular unconformity in other sectors of the Neuquén Basin (Groeber 1946; Ramos and Folguera 2005). Internal angular and erosive unconformities are common in the lower Neuquén Group deposits west of the Cara Cura anticline (Fig. 6b), whose clastic composition is dominated by limestone
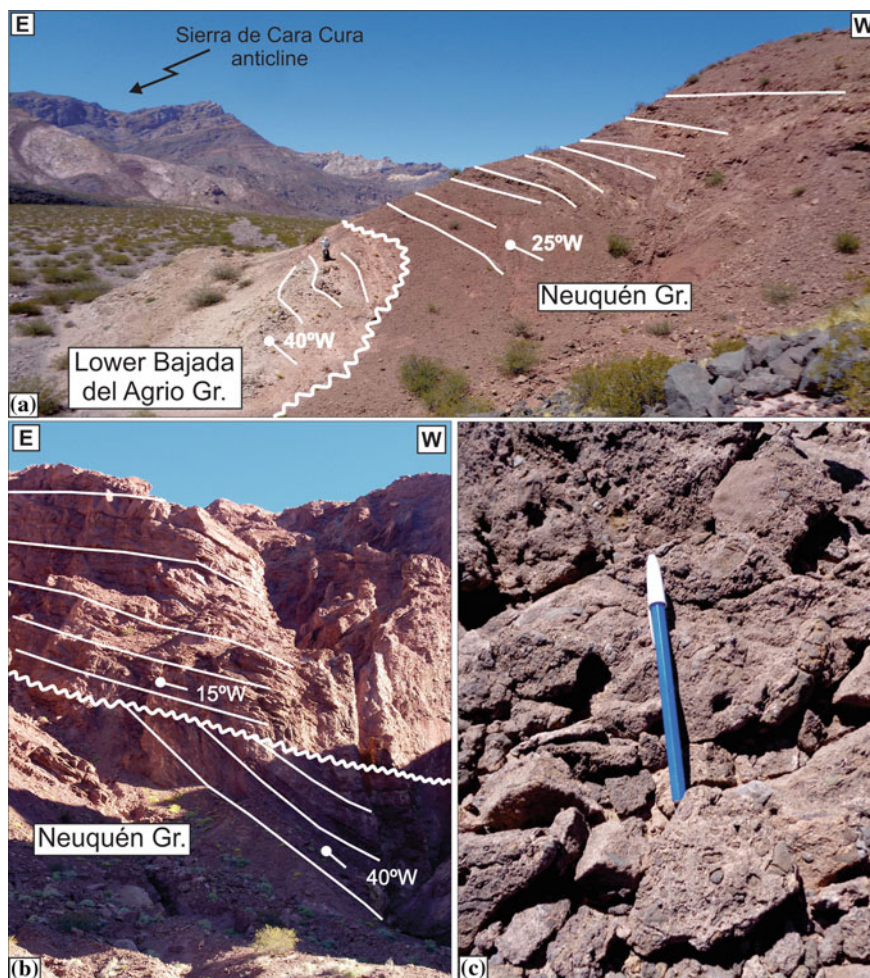

Fig. 6 **a** View of the angular unconformity between the lower terms of the Bajada del Agrio Group and the red beds of the Neuquén Group west of the Cara Cura anticline. **b** Internal erosive and angular unconformities in the lower terms of the Neuquén Group adjacent to the Cara Cura anticline. **c** The coarse facies of the lower Neuquén Group in the vicinities of the Cara Cura anticline are mainly composed by limestone clasts

pebbles (Fig. 6c), in accordance with sandstone petrographic analyses (Fennell et al. 2017b).

Moving southwards, the Chihuido anticline (Fig. 2) appears as another important Late Cretaceous structure in the eastern sector, where the angular unconformity between the deposits of the Neuquén and Bajada del Agrio Groups was first described (Groeber 1946; Ramos and Folguera 2005). In this area, deformational and liquefaction structures are interpreted as seismetes, whose nature and distribution suggest they were triggered by earthquakes of >6 magnitude in the Richter scale (Sánchez et al. 2013).

5   Late Cretaceous Orogenic Erosion and Structural Domains

The structures grouped into the western, central and eastern sectors present defined structural characteristics during the deposition of the Neuquén Group, which allow their separation into different structural domains. Structures in the western sector present evidences of non-deposition or exhumation due to active erosion during Late Cretaceous times, as highlighted by the presence of a long-lasting hiatus and important angular unconformities, which are among the most direct consequences of tectonic uplift. Orogenic erosion can be analysed through thermochronology, which is based on the production of an isotope or radiation damage in minerals such as apatites and zircons, reflecting the path taken by a particular rock in its way to the surface (Reiners and Brandon 2006). One of the most popular thermochronologic methods are the apatite fission track analyses (AFTA), which have been performed in some of the structures located in the western sector, revealing cooling ages between ~70 and 40 Ma (Fig. 7) (Folguera et al. 2015; Rojas Vera et al. 2015). Moreover, an Ar/Ar cooling age obtained from a pluton intruding the Cordillera del Viento anticline has been interpreted as the product of a 6 km tectonic uplift (Fig. 7) (Kay et al. 2006), in accordance with AFTA recently performed in this structure (Sánchez et al. 2018) (see Chapter "Structural and thermochronological constraints on the exhumation of the Chos Malal fold and thrust belt ~37º S"). Since erosion usually follows rock and surface uplift in space and time, the cooling ages obtained from the AFTA and Ar/Ar dating in the western structures could be reflecting their erosion after their initial growth (Reiners and Brandon 2006).

The central sector groups structures where thickness variations and progressive unconformities have been described during the deposition of the Neuquén Group. These evidences suggest that structural uplift occurred coeval to sedimentation, which might have resulted in positive topographic features affecting the local drainage patterns during brief periods of time. In this case, the only structure targeted for AFTA was the Bardas Blancas anticline (Fig. 7), with cooling ages spanning a wide temporal range between 120 and 52 Ma (Folguera et al. 2015), which might indicate active erosion during and/or after deposition of the Neuquén Group.
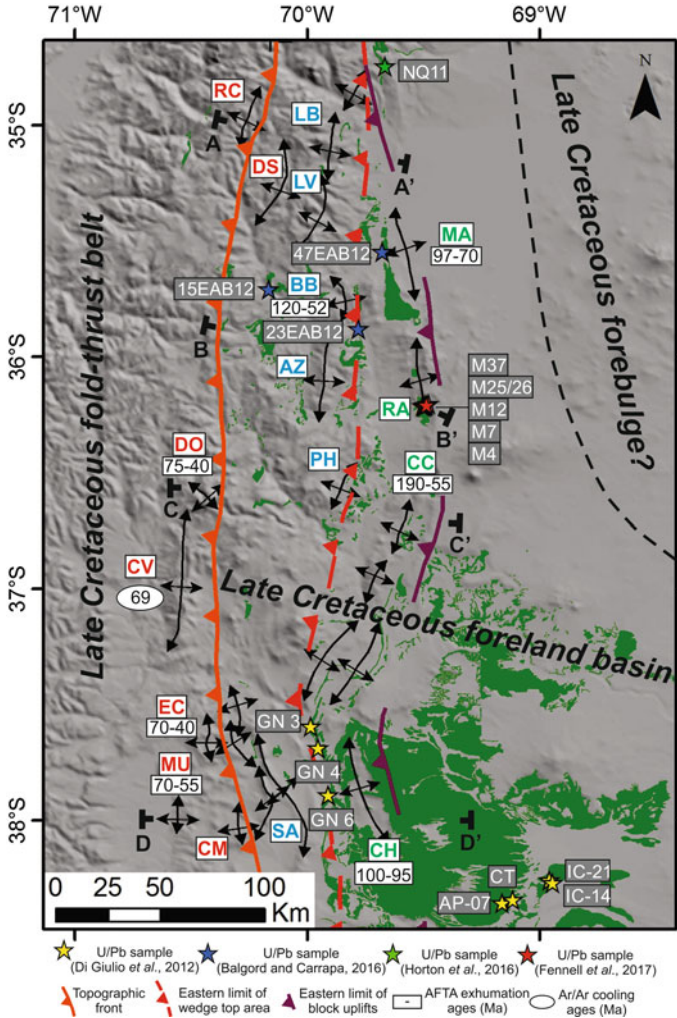
Fig. 7 The Late Cretaceous foreland basin system was characterized by a western sector of exhumed and actively eroded structures, which sourced sediments to the foreland basin, where structures were growing below the level of sedimentation after the eastern migration of the forebulge up to a position that would have coincided with the current location of the San Rafael Block. Abbreviations of the main structures are the same as in Fig. 2

On the other hand, structures located in the eastern sector show punctuated uplift events and limited amount of erosion, highlighted by mild angular unconformities between the Bajada del Agrio and Neuquén Group deposits. These structures are isolated, and seem to have been only active during the deposition of the lower terms of the Neuquén Group. These observations are supported by AFTA performed in some of these structures such as the Malargüe, Cara Cura and Chihuido anticlines

(Fig. 7), where cooling ages overlap with evidences of Late Cretaceous contractional deformation (Zamora Valcarce et al. 2009; Folguera et al. 2015). However, it should be noted that although the Malargüe anticline does not show any direct evidence of Late Cretaceous uplift, the fault responsible for its growth shows minor displacements both to the north in the Río Atuel area (Boll et al. 2014) and to the south in the La Batra area (Fennell et al. 2017a).

6 Late Cretaceous Detrital Zircon Provenance and Source Areas

Changes in detrital source areas are considered as an indirect evidence of change in the regional slope affecting the basins paleodrainage, which can be linked to rock exhumation in response to tectonic uplift. In order to study these provenance polarity reversals, the U–Pb dating of detrital zircons gained relevance during the last few years in the Neuquén Basin, since the pioneering study of Tunik et al. (2010). This study compared the U–Pb age patterns of detrital zircons of the Lower and Upper Cretaceous units, showing that eastern provenance characterized the zircons of the Bajada del Agrio Group, while western provenance dominated the zircons of the Neuquén Group. This study was later complemented by Di Giulio et al. (2012) at 38° S (Fig. 7), who show a second polarity reversal towards the top of the Neuquén Group, associated with the growing importance of the eastern source areas once the Late Cretaceous fold-thrust belt entered a mature phase. However, the replication of this type of analyses by Balgord and Carrapa (2016) at 36° S (Fig. 7) arrived to a different result, since a constant western provenance is recorded throughout the deposits of the Bajada del Agrio and Neuquén Groups. These apparent contradictory results were supported by AFTA performed by Di Giulio et al. (2017) in detrital apatites from the Neuquén Group, which reported Cretaceous cooling ages independent on their U–Pb crystallization ages (Fig. 8a). These observations led Fennell et al. (2017a) to propose that the detrital zircon provenance in the Neuquén Group also responds to the position of the sample within the basin, which they supported with a complete set of U–Pb age patterns of detrital zircons from the Ranquil Co anticline showing no time-dependant source variations (Fig. 7).

In order to understand these spatio-temporal variations, it is important to note that source areas of zircons with U–Pb ages younger than ~200 Ma can only be found west of the basin or be directly sourced from the coeval magmatic arc, sources of ~200–400 Ma zircons are ubiquitous along the basin, and zircons older than ~400 Ma are only sourced from the eastern cratonic area (Naipauer and Ramos 2016). Nevertheless, since the deposits of the Neuquén Group are also a consequence of the erosion of the Neuquén basin's sedimentary infill, zircon recycling is another important process that should be taken into account. In consequence, the Late Cretaceous foreland basin can be divided into different areas showing a distinct U–Pb age pattern of detrital zircons (Fig. 8).
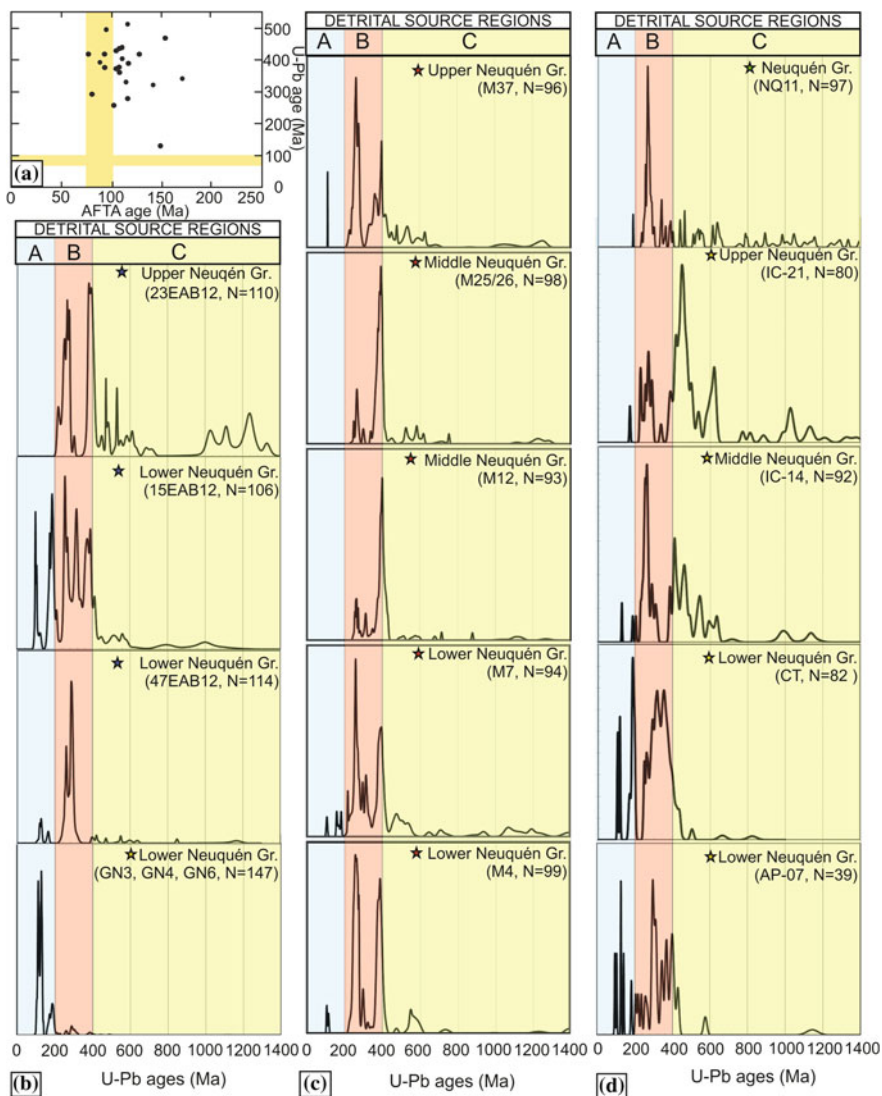
Fig. 8 **a** AFTA and U–Pb dating of detrital apatites show that the Neuquén Group detritus (depositional age highlighted in yellow) are the consequence of erosion during Cretaceous times, independently on their crystalization age (error bars not included, taken and modified from Di Giulio et al. 2017). **b** Samples in the westernmost sector of the basin were sourced from the west, and show an increasing level of exhumation throughout the section (taken and modified from Di Giulio et al. 2012 and Balgord and Carrapa 2016). **c** Samples located in a central position show a predominance of 200–400 Ma zircons, whose sources are ubiquitous along the basin (taken and modified from Fennell et al. 2017a). **d** U–Pb age patterns of detrital zircons from samples located east of growing structures show an initial western detrital derivation, which gradually changes towards an eastern derivation, indicating an increasing importance of the cratonic sources once the Late Cretaceous fold-thrust belt enters its mature phase (taken and modified from Di Giulio et al. 2012 and Horton et al. 2016). Location of all the U–Pb samples is given in Fig. 7

The westernmost samples (Fig. 8b) are characterized by a western detrital derivation, with their lower terms receiving zircons younger than 200 Ma, being gradually replaced to the top by zircons with U–Pb ages between 200 and 400 Ma (Fig. 8b) (Tunik et al. 2010; Balgord and Carrapa 2016). The upper Neuquén Group shows the appearance of zircon grains older than 400 Ma (Fig. 8b) (Balgord and Carrapa 2016), indicating an uplifted topographic barrier inhibiting western detrital derivation, or increasing exhumation and recycling from older sedimentary units, which agree with the description of their clastic components (Borghi et al. 2017). A second set of samples are characterized by detritus coming from mixed sources with a fairly constant U–Pb age pattern of detrital zircons from base to top (Fig. 8c) (Fennell et al. 2017a). These patterns show the dominance of 200–400 Ma old zircons, whose source areas can be found either to the east or west of the basin (Naipauer and Ramos 2016), with little input from younger and older sources, which can be interpreted as recycling of underlying sedimentary units (Fennell et al. 2017a). Finally, the easternmost samples are characterized by a strong input from western sources in its base, reflected by the abundant zircons younger than 200 Ma (Fig. 8d) (Di Giulio et al. 2012). Later on, a reversal in provenance is recorded towards the upper Neuquén Group deposits, when zircons older than 400 Ma start to dominate, evidencing an important contribution from eastern sources (Fig. 8d) (Di Giulio et al. 2012; Horton et al. 2016).

7 The Late Cretaceous Orogenic System

Through the study of present foreland basin systems worldwide, it has been shown that these include four discrete areas that reflect particular sedimentological and structural conditions, which are referred to as the wedge-top, foredeep, forebulge and back-bulge depozones (DeCelles and Giles 1996; DeCelles 2012). In the case of the Late Cretaceous foreland basin between 35° and 38° S, the present level of understanding allows the identification of each of these areas, showing striking similarities with modern Andean foreland basins (Horton 2018b).

The wedge-top depozone includes the mass of sediment that accumulates on top of the frontal part of the orogenic wedge, which is characterized by the presence of growth strata, tectonic unconformities and derivation of immature sediments from the fold-thrust belt (DeCelles and Giles 1996; DeCelles 2012; Capaldi et al. 2017). In the Late Cretaceous foreland basin, the structures described in the western sector correspond to the frontal part of the orogenic wedge, marking the topographic front during deposition of the Neuquén Group (Fig. 7). Structures in the central sector correspond to structures growing below the level of sedimentation in the wedge-top depozone accumulating textural and compositional immature detritus (Fig. 7), resulting in important thickness variations, progressive unconformities and evidences of syndepositional deformation.

The foredeep depozone consists of the cratonicward tapering wedge of sediment derived predominantly from the fold-thrust belt, with minor contributions from the stable craton (DeCelles and Giles 1996; DeCelles 2012; Capaldi et al. 2017).

Although this depozone is usually characterized as tectonically inactive, in areas with pre-existing heterogeneities inherited from former tectonic events, fault reactivation leading to basement block uplifts appears as an additional feature (e.g., Jordan and Allmendinger 1986; Mitra and Mount 1998; Ramos et al. 2002). Such structures should have been common in the Late Cretaceous foreland basin given the wide variety of pre-existing structures (Manceda and Figueroa 1995; Bechis et al. 2014), although their presence in the Late Cretaceous geological record has been underestimated. Structures present in the eastern sector could have behaved as disconnected basement block uplifts during the Late Cretaceous (Fig. 7), since they correspond to inverted structures with a punctuated uplift event during the initial stages of synorogenic sedimentation. The synchronicity in the uplift of these structures could be explained by a first stage of early fault inversion throughout the entire Neuquén Basin. This early basin inversion was later deactivated and followed by the development of the fold-thrust belt to the west, in agreement with results obtained from analogue modelling of tectonic inversion of former extensional sedimentary basins (e.g., Amilibia et al. 2005; Bonini et al. 2012).

The forebulge depozone corresponds to the region of potential flexural uplift along the cratonic side of the foredeep, usually characterized by condensed stratigraphic sections or low-angle unconformities that are used to track its position through time (Decelles and Giles 1996; DeCelles 2012). Balgord and Carrapa (2016) interpret the passage of the forebulge based on a 25–30 Myr unconformity between the lower terms of the Bajada del Agrio Group and the Neuquén Group, while foredeep and forebulge geometries have been interpreted in an area located east of the basement block uplift area towards the middle terms of the Neuquén Group (Sánchez and Asurmendi 2014). Sánchez and Asurmenti (2014) also detect periods of substantial detrital influx coming from the fold-thrust belt to the west, which is a common feature of distal foredeep and forebulge areas (DeCelles 2012). Although the final position of the forebulge is unknown, the isopach map of the Neuquén Group suggests that the position of the forebulge between 35º and 38º S would have coincided with the current position of the San Rafael Block (Figs. 2 and 7). In this context, the back-bulge deposits are represented by the Bajada del Agrio Group, which are found partially or completely eroded due to the passage of the forebulge before deposition of the Neuquén Group.

Since all the components of the Late Cretaceous foreland basin system have been identified, the Late Cretaceous orogenic system between 35º and 38º S can be schematized based on a series of previously published structural sections (Fig. 9) (Orts et al. 2012; Mescua et al. 2014; Folguera et al. 2015; Rojas Vera et al. 2015).

In the northernmost section, located at ~35º S (Fig. 7), the frontal part of the fold-thrust belt is represented by the Río del Cobre anticline, and the wedge-top area by the Dedos Silla anticline, where the clastic components indicate exhumation of Late Jurassic and Early Cretaceous units to the west (Fig. 9) (Mescua et al. 2013). The transition towards the foredeep in this area is not clearly defined, although clastic provenance in the eastern Neuquén Group outcrops indicates erosion of a peripheral bulge located further east (Mescua et al. 2013), where evidence of active thrusting involving the basement has been hinted through seismic sections by Boll et al. (2014).
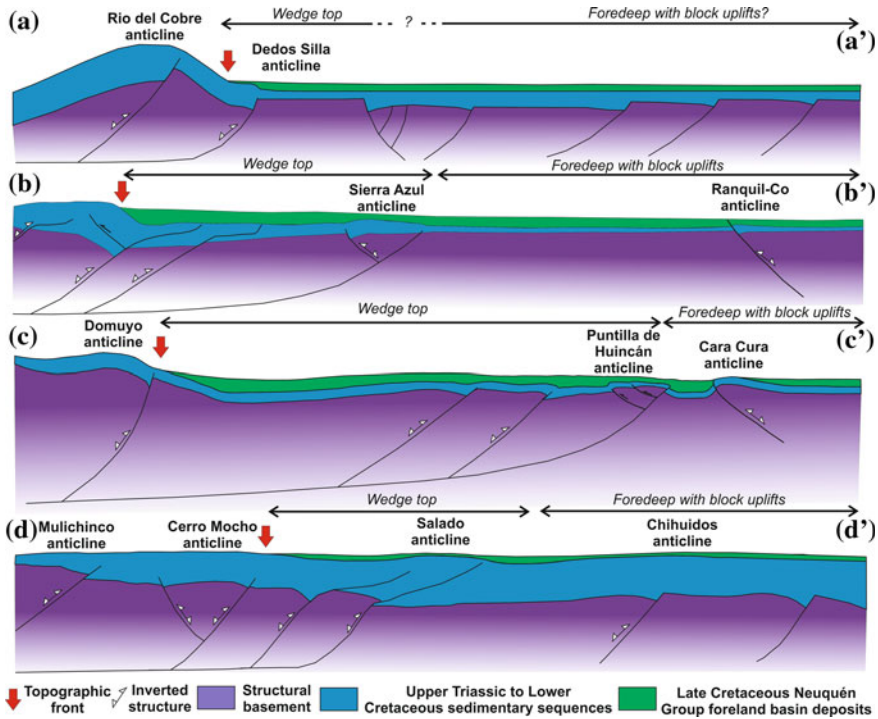
Fig. 9 Schematic representation of the Late Cretaceous orogenic system between 35° and 38° S through a series of published structural sections (A–A′ from Mescua et al. 2014; B–B′ from Orts et al. 2012; C–C′ from Folguera et al. 2015; D–D′ from Rojas Vera et al. 2015). Location of the structural cross sections is given in Fig. 7

The structural section performed around 36° S (Fig. 7) shows the Sierra Azul anticline as part of the wedge-top area (Fig. 9), receiving sediments from the fold-thrust belt to the west, as evidenced by the complete unroofing sequence detected in the outcrops of the Neuquén Group in this area (Borghi et al. 2017). The Ranquil Co anticline in the eastern sector of the section would represent a basement block uplift within the foredeep area, deforming strata from the Neuquén Group sourced from both the eastern cratonic area and the active fold-thrust belt to the west (Fig. 9).

At 37° S (Fig. 7), the exhumed and actively eroded frontal part of the Cretaceous orogenic wedge is represented by the Domuyo anticline, defining a wide wedge-top area including the Puntilla del Huincán anticline (Fig. 9). To the east, the Cara Cura anticline would have been disconnected from the main decollement and would have been active only during the initial stages of contractional deformation, being partially eroded and sourcing the limestone clasts to the western depocentre (Fig. 9).

Finally, the southern section at 38° S (Fig. 9) shows the exhumation of the Mulichinco and Cerro Mocho anticlines in the inner sector, the growth of the Salado anticline

in the wedge-top area, and the Chihuidos anticline as a basement block uplift in the eastern foredeep area (Fig. 9).

A general analysis of the Late Cretaceous orogenic system indicates that inversion mechanisms were predominant along the uplifted structures, which can be separated into a group of connected structures growing in the fold-thrust belt and wedge-top areas, and a group of isolated structures acting as basement block uplifts in the foredeep depozone (Fig. 9). The effect of this contractional stage outlined the present structural framework between 35º and 38º S, being its impact in the geological record more intense towards the southern structures, in agreement with a regional trend of increasing deformation during Late Cretaceous times towards higher latitudes along the Andes (see Gianni et al. 2018).

References

Álvarez Cerimedo J, Orts DL et al (2013) Mecanismos y fases de construcción orogénicos del frente oriental andino (36º S, Argentina). Andean Geol 40(3):504–520

Amilibia A, McClay KR, Sábat F et al (2005) Analogue modelling of inverted oblique rift systems. Geol Acta 3(3):251–271

Balgord EA, Carrapa B (2016) Basin evolution of upper Cretaceous-lower cenozoic strata in the Malargüe fold-and-thrust belt: northern Neuquén Basin, Argentina. Basin Res 28(2):183–206

Barrio CA (1990) Paleogeographic control of the upper Cretaceous tidal deposits, Neuquén Basin, Argentina. J S Am Earth Sci 3(1):31–49

Bechis F, Cristallini EO, Giambiagi LB et al (2014) Transtensional tectonics induced by oblique reactivations of previous lithospheric anisotropies during the Late Triassic to Early Jurassic rifting in the Neuquén basin: insights from analog models. J Geodynamics 79:1–17

Bettini FH, Pombo RA, Mombru CA et al (1978) Consideraciones sobre el diastrofismo andino en la vertiente oriental de la cordillera principal entre los 34°30′ y los 37º de latitud sur. In: Abstracts of the 7 Congreso Geológico Argentino, Neuquén, 5–9 Nov 1978

Boll A, Alonso J, Fuentes F et al (2014) Factores controlantes de las acumulaciones de hidrocarburos en el sector norte de la cuenca neuquina, entre los ríos Diamante y Salado, provincia de Mendoza, Argentina. In: Abstracts of the 9 Congreso de Exploración y Desarrollo de Hidrocarburos, Mendoza, 3–4 Nov 2014

Bonini M, Sani F, Antonielli B (2012) Basin inversión and contractional reactivation of inherited normal faults: a review based on previous and new experimental models. Tectonophysics 522–523:55–88

Borghi P, Gómez Omil R, Fennell L et al (2017) Nuevas evidencias del levantamiento del sur de los Andes Centrales (36º S) durante la depositación del Grupo Neuquén. In Abstracts of the 20 Congreso Geológico Argentino, San Miguel de Tucumán, 7–11 Aug 2017

Branellec M, Niviere B, Callot JP et al (2016) Mechanisms of basin contraction and reactivation in the basement-involved Malargüe fold-and-thrust belt, Central Andes (34–36° S). Geol Mag 153(5/6):926–944

Capaldi TN, Horton BK, McKenzie NR et al (2017) Sediment provenance in contractional orogens: the detrital zircon record from modern rivers in the Andean fold-thrust belt and foreland basin of western Argentina. Earth Planet Sci Lett 479:83–97

Cobbold PR, Rosello EA (2003) Aptian to recent compressional deformation, foothills of the Neuquén Basin, Argentina. Marine Petrol Geol 20:429–443

DeCelles PG (2012) Foreland basin systems revisited: variations in response to tectonic settings. In: Busby C, Azor A (eds) Tectonics of sedimentary basins: recent advances. Wiley-Blackwell, Oxford, pp 405–426

DeCelles PG, Giles KA (1996) Foreland basin systems. Basin Res 8(2):105–123

Di Giulio A, Ronchi A, Sanfilippo A et al (2012) Detrital zircon provenance from the Neuquén Basin (south-central Andes): Cretaceous geodynamic evolution and sedimentary response in a retroarc-foreland Basin. Geology 40:559–562

Di Giulio A, Ronchi A, Sanfilippo A et al (2017) Cretaceous evolution of the Andean margin between 36º S and 40º S latitude through a multi-proxy provenance analysis of Neuquén Basin strata (Argentina). Basin Res 29(3):284–304

Fennell LM, Folguera A, Naipauer M et al (2017a) Cretaceous deformation of the southern Central Andes: synorogenic growth strata in the Neuquén Group (35º 30′–37º S). Basin Res 29(S1):51–72

Fennell LM, Naipauer M, Folguera A (2017b) El movimiento Intersenoniano de Pablo Groeber en el norte de Neuquén y sur de Mendoza: bases de la primera orogenia andina. Rev Asoc Geol Argentina 74(1):59–73

Fennell LM, Iannelli SB, Folguera A et al (2017) Interrupciones extensionales en el desarrollo de la faja plegada y corrida de Malargüe (36º S). In: Abstarcts of the 20 Congreso Geológico Argentino, San Miguel de Tucumán, 7–11 Aug 2017

Folguera A, Bottesi G, Duddy I et al (2015) Exhumation of the Neuquén Basin in the southern Central Andes (Malargüe fold and thrust belt) from field data and low-temperature thermochronology. J S Am Earth Sci 64(2):381–398

Folguera A, Naipauer M, Sagripanti L et al (2016) An introduction to the Southern Andes (33–50º S): Book structure. In: Folguera A, Naipauer M, Sagripanti L, Ghiglione M, Orts DL, Giambiagi L (eds) Growth of the Southern Andes. Springer, pp 1–7

Galarza BJ, Zamora Valcarce G, Folguera A et al (2009) Geología y Evolución tectónica del Frente Cordillerano a los 36º 30′ S: bloques de Yihuin-Huaca y Puntilla de Huincán. Mendoza. Rev Asoc Geol Argent 65(1):170–191

Gianni GM, Dávila FM, Echaurren A et al (2018) A geodynamic model linking Cretaceous orogeny, arc migration, foreland dynamic subsidence and marine ingression in southern South America. Earth-Sci Reviews 185:437–462

Groeber P (1946) Observaciones Geológicas a lo largo del meridiano 70: 1. Hoja Chos Malal. Rev Asoc Geol Argent 1(3):117–208

Groeber P (1947) Observaciones geológicas a lo largo del meridiano 70: 3, Hojas Domuyo, Mari Mahuida, Huarhuar-co y parte de Epu Lauken, 4, Hojas Bardas Blancas y Los Molles. Rev Asoc Geol Argent 2(4):347–433

Horton BK (2018a) Tectonic regimes of the central and southern Andes: responses to variations in plate coupling during subduction. Tectonics 37:402. https://doi.org/10.1002/2017TC004624

Horton BK (2018b) Sedimentary record of Andean mountain building. Earth-Sci Rev 178:279–309

Horton BK, Fuentes F, Boll A et al (2016) Andean stratigraphic record of the transition from backarc extension to orogenic shortening: a case study from the northern Neuquén Basin, Argentina. J S Am Earth Sci 71:17–40

Iannelli SB, Fennell LM, Litvak VD et al (2018) Geochemical and tectonic evolution of Late Cretaceous to early Paleocene magmatism along the Southern Central Andes (35–36º S). J S Am Earth Sci. https://doi.org/10.1016/j.jsames.2017.12.008

Jordan TE, Allmendinger RW (1986) The Sierras Pampeanas of Argentina: a modern analogue of rocky mountain foreland deformation. Am J Sci 286:737–764

Jordan TE, Burns WM, Veiga R et al (2001) Extension and basin formation in the southern Andes caused by increased convergence rate: a mid-Cenozoic trigger for the Andes. Tectonics 20(3):308–324

Kay SM, Burns M, Copeland P (2006) Upper Cretaceous to Holocene magmatism and evidence for transient Miocene shallowing of the Andean subduction zone under the northern Neuquén Basin. In: Kay SM, Ramos VA (eds) Evolution of an Andean margin: a tectonic and magmatic view from the Andes to the Neuquén Basin (35–39º S). Geol Soc Am, SP 407, pp 19–60

Legarreta L, Kozlowski E (1984) Secciones condensadas del Jurásico-Cretácico de los Andes del sur de Mendoza: estratigrafía y significado tectosedimentario. In: abstracts of the 9 Congreso Geológico Argentino, San Carlos de Bariloche, 5–89 Nov 1984

Llambías EJ, Leanza HA, Carbone O (2007) Evolución tectono-magmática durante el Pérmico al Jurásico Temprano en la Cordillera del Viento (37° 05′ S–37° 15′ S): nuevas evidencias geológicas y geoquímicas del inicio de la cuenca Neuquina. Rev Asoc Geol Argentina 62(2):217–235

Manacorda L, Reinante SME, Cazau L, Penna E (2002) Los reservorios del Grupo Neuquén. Abstracts of the V Congreso de Exploración y Desarrollo de Hidrocarburos, Mar del Plata, 29 Oct–2 Nov 2002

Manceda R, Figueroa D (1995) Inversion of the Mesozoic Neuquén rift in the Malargüe fold and thrust belt, Mendoza, Argentina. In: Tankard AJ, Suárez R, Welsink HJ (eds) Petroleum basins of South America. AAPG Memoir, vol 62, pp 369–382

Mescua JF, Giambiagi LB, Ramos VA (2013) Late Cretaceous uplift in the Malargüe fold-and-thrust belt (35º S), southern Central Andes of Argentina and Chile. Andean Geol 40(1):102–116

Mescua JF, Giambiagi LB, Tassara A et al (2014) Influence of pre-Andean history over Cenozoic foreland deformation: structural styles in the Malargüe fold-and-thrust belt at 35º S, Andes of Argentina. Geosphere 10(3):585–609

Mitra S, Mount VS (1998) Foreland basement-involved structures. AAPG Bulletin 82(1):70–109

Naipauer M, Ramos VA (2016) Changes in source areas at Neuquén basin: mesozoic evolution and tectonic setting based on U–Pb ages on zircons. In: Folguera A, Naipauer M, Sagripanti L et al (eds) Growth of the Southern Andes. Springer, New York, pp 33–61

Orts DL, Folguera A, Giménez M et al (2012) Variable structural controls through time in the Southern Central Andes (~36º S). Andean Geol 39(2):220–241

Parras A, Griffin M (2013) Late Cretaceous (Campanian/Maastrichtian) freshwater to restricted marine mollusk fauna from the Loncoche Formation, Neuquén Basin, west-central Argentina. Cretaceous Res 40:190–206

Ramos VA (1981) Descripción geológica de la Hoja 33 c Los Chihuidos Norte, provincia del Neuquén. Bol Serv Geol Nac 182:1–103

Ramos VA, Folguera A (2005) Tectonic evolution of the Andes of Neuquén: constraints derived from the magmatic arc and foreland deformation. In: Veiga GD, Spalletti LA, Howell JA et al (eds) The Neuquén Basin, Argentina: a case study in sequence stratigraphy and basin dynamics. Geol Soc, London, SP, vol 252, pp 15–35

Ramos VA, Cristallini EO, Pérez DJ (2002) The Pampean flat-slab of the Central Andes. J S Am Earth Sci 15:59–78

Reiners PW, Brandon MT (2006) Using thermochronology to understand orogenic erosion. Annu Rev Earth Planet Sci 34:419–466

Rojas Vera EA, Mescua J, Folguera A et al (2015) Evolution of the Chos Malal and Agrio fold and thrust belts, Andes of Neuquén: insights from structural analysis and apatite fission track dating. J S Am Earth Sci 64:418–433

Sagripanti L, Bottesi G, Naipauer M et al (2011) U/Pb ages on detrital zircons in the southern central Andes Neogene foreland (36º–37º S): constraints on Andean exhumation. J S Am Earth Sci 32(4):555–566

Sagripanti L, Folguera A, Fennell L et al (2016) Progression of the deformation in the Southern Central Andes (37º S). In: Folguera A, Naipauer M, Sagripanti L, Ghiglione M, Orts DL, Giambiagi L (eds) Growth of the Southern Andes. Springer, New York, pp 115–132

Sánchez ML, Asurmendi E (2014) Modelo de depósito de la Formación Cerro Lisandro: lóbulos de desembocadura y deltas de tipo Gilbert. Cretácico superior, región central de cuenca Neuquina, Argentina. Rev Mex Cs Geol 31(2):141–162

Sánchez ML, Asurmendi E, Armas P (2013) Subgrupo Río Colorado (Grupo Neuquén): registros de paleosismicidad en la cuenca de antepaís andina, Cuenca Neuquina, Provincias de Neuquén y Río Negro. Rev Asoc Geol Argent 70(1):96–114

Sánchez NP, Coutand I, Turienzo M et al (2018) Tectonic evolution of the Chos Malal fodl.and.thrust belt (Neuquén Basin, Argentina) from (U-Th)/He and fission track thermochronometry. Tectonics 37:1907–1929. https://doi.org/10.1029/2018tc004981

Silvestro J, Zubiri M (2008) Convergencia Oblicua: Modelo estructural alternativo para la dorsal neuquina (39º S)—Neuquén. Rev Asoc Geol Argent 63(1):49–64

Silvestro J, Atencio M (2009) La cuenca Cenozoica del Río Grande y Palauco: Edad, evolución y control estructural, faja plegada de Malargüe (36º S). Rev Asoc Geol Argent 65(1):154–169

Silvestro J, Kraemer P, Achilli F et al (2005) Evolución de las cuencas sinorogéncias de la Cordillera Principal entre 35º–36º S, Malargüe. Rev Asoc Geol Argent 60(4):627–643

Tunik M, Folguera A, Naipauer M et al (2010) Early uplift and orogenic deformation in the Neuquén Basin: Constraints on the Andean uplift from U–Pb and Hf isotopic data of detrital zircons. Tectonophysics 489:258–273

Vergani GD, Tankard J, Belotti J et al (1995) Tectonic evolution and paleogeography of the Neuquén basin, Argentina. In: Tankard AJ, Suárez R, Welsink HJ (eds) Petroleum Basins of South America. AAPG Memoir, vol 62, pp 383–402

Zamora Valcarce G, Zapata T, Ramos VA et al (2009) Evolución tectónica del frente andino en Neuquén. Rev Asoc Geol Argent 65(1):192–203